ginning of the x-ray trace before the large pulse is a small amount of beam injected in the opposite direction to the main beam.) (5) The trapped signals on the individual magnetic probes sometimes showed individual peaks at 60–80-nsec intervals as shown in Fig. 3.

Point one indicates that there was enough primary beam trapped to keep the net current rising after the initial beam pulse. Point two indicates that even though the decay rates of the trapped and untrapped shots do not differ appreciably, the decay of the trapped beam included primary beam current whereas the untrapped decay did not. Point three indicates the presence of a dip in the beam current. This implies that the once-around propagation time is long enough to avoid any possible head-tail interaction. Point four indicates that there was a distinct head to the beam and it remained intact for at least three transits.

The characteristics of the trapped beam listed above were evident in most shots. The decay times of the x-ray signals and calculated net currents varied from shot to shot but the best conditions for confinement appeared to be at 200 $\mu$m and 3.8 kG. Magnetic fields in excess of 5 kG can now be obtained and experiments to lengthen the confinement time are underway. Indications are that confinement time may lengthen with higher magnetic fields since injection and propagation improve with field strength. In addition there is evidence that effects other than collisions are limiting the confinement time. These effects may be associated with geometry, and minor modifications to the experiment are currently under consideration.

The data taken to date prove that the injection and trapping of an intense relativistic electron beam can be accomplished with the field-shaping cathodes described. This technique provides a mechanism for injecting large amounts of energy into a toroidal system with a high magnetic field.

The authors would like to acknowledge the help of Milt Johnson in running the experiment.

*Research supported by Electric Power Research Institute under Contract No. RP-108.

†On leave from the Weizmann Institute of Science, Rehovot, Israel.

[1]D. F. Brower, B. R. Kusse, and G. D. Meixel, Jr., IEEE Trans. Plasma Sci. 2, No. 3, 193 (1974).

[2]P. Gilad, B. R. Kusse, and T. Lockner, "Injection and Drift Studies of High-Current Relativistic Electron Beams into a Toroidallike System" (to be published).

[3]G. J. Meixel, Jr., P. Gilad, and B. R. Kusse, Bull. Amer. Phys. Soc. 18, 1284 (1973).

[4]D. A. Hamner and N. Rostoker, Phys. Fluids 13, 1831 (1970).

[5]J. J. Lee and R. N. Sudan, Phys. Fluids 14, 1213 (1971).

[6]K. R. Chu and N. Rostoker, Phys. Fluids 16, 1472 (1973).

[7]D. A. McArthur and J. W. Poukey, Phys. Fluids 16, 1996 (1973).

# Intense Coherent Cherenkov Radiation Due to the Interaction of a Relativistic Electron Beam with a Slow-Wave Structure

Y. Carmel, J. Ivers, R. E. Kribel, and J. Nation
*Laboratory of Plasma Studies, Cornell University, Ithaca, New York 14853*
(Received 25 July 1974)

Extremely high-power microwave emission is generated when a pulsed relativistic electron beam propagates down the axis of a corrugated-wall wave guide. The radiation occurs at a frequency such that the phase velocities of the negative-energy space charge wave on the beam and a low-order TM mode in the wave guide are equal. Power levels of 500 MW are generated. The conversion efficiency of electron energy into electromagnetic energy radiation is 17%.

One of the promising applications of relativistic electron beams is in the generation of very high-power microwave pulses.[1] Recently schemes involving cyclotron radiation processes have been investigated[2-9] both experimentally and theoretically. Although these processes are effective, the conversion efficiencies of electron energy to electromagnetic energy are limited to 1–2%. A major limitation of the cyclotron processes is the requirement that the electron beam possess perpendicular energy in some form, i.e., either anisotropy or temperature inversion.

An alternative, potentially more efficient scheme was reported in 1970 by Nation[1] in which an intense relativistic electron beam was coupled to a capacitively loaded wave guide (slow-wave structure). The radiation power can be increased appreciably, compared to high-power klystrons, through a matched increase in electron energy and beam current. In Nation's experiment a power level of 10 MW and a conversion efficiency of 0.05% were measured in the 3-cm band. [For comparison, low-power backward wave oscillators (BWO) have efficiencies of about 30%.] The relatively low conversion efficiencies observed were attributed to microwave breakdown in the large electric fields (~15 KV/cm) associated with the radiation and enhanced by the shape of the slow-wave structure.

In 1973, Kovalev *et al.*[10] achieved conversion efficiencies of 12–15% by coupling a relativistic electron beam to an inductively loaded wave guide (slow-wave structure). However, very little information is given about the absolute power levels, the frequency spectrum, or the experimental configuration.

In the work described in this paper we have observed microwave power levels of 500 MW and conversion efficiencies of 17%. A pulsed (70 nsec) relativistic electron beam propagates along the axis of a slow-wave structure consisting of a corrugated-wall wave guide as shown in Fig. 1. The energy content of the microwave pulse produced by this device can be increased by (a) increasing the pulse width to a few microseconds and (b) operating at higher electron energies. A repetitive machine is also within the state of the art. High-power microwave sources of this type may be used for (1) plasma heating, (2) nonthermal biological effects research, and (3) generating intense infrared radiation by upconversion of the microwave signal through scattering from the electron beam.[11]

A Blumlein electron accelerator coupled to a foilless diode has been used to produce a solid-pencil electron beam, 1 cm in diameter, whose parameters are given below:

| Beam injection energy (keV) | Beam injection current (kA) | Calculated[12] max drift current (kA) | Reduced[13] beam plasma frequency ($cm^{-3}$) |
|---|---|---|---|
| 500–900 | 2–15 | 1.8–5 | $10^{11}$ |

The electron injector impedance (see table) is 60–200 Ω. An electron beam traveling with velocity $V_0$ can support, in the absence of the structure, slow space charge waves with phase velocities

$$V_p = \omega/k = V_0/[1 + (\omega_p/\omega\gamma)], \tag{1}$$

where $\omega$, $\omega_p$, and $k$ are the angular frequency, reduced plasma frequency, and axial wave number, respectively, of the wave supported by the beam, while $\gamma$ is the relativistic factor given by $\gamma = (1-\beta^2)^{-1/2}$. The vacuum properties of the corrugated-wall wave guide were approximated by the disk-loaded waveguide dispersion relation[14]

$$c^2 I_1\left(ak^2 - \frac{a}{c^2}\omega\right)\left[\left(ak^2 - \frac{a}{c^2}\omega^2\right) a I_0\left(ak^2 - \frac{a}{c^2}\omega^2\right)\right]^{-1}$$
$$= \frac{c}{\omega a}\left[J_1\left(\frac{\omega}{c}a\right)N_0\left(\frac{\omega}{c}b\right) - N_1\left(\frac{\omega}{c}a\right)J_0\left(\frac{\omega}{c}b\right)\right]\left[J_0\left(\frac{\omega}{c}a\right)N_0\left(\frac{\omega}{c}b\right) - N_0\left(\frac{\omega}{c}a\right)J_0\left(\frac{\omega}{c}b\right)\right]^{-1}. \tag{2}$$

In the above equation $J$, $N$, and $I$ are Bessel functions; $\omega$ and $k$ represent the angular frequency and wave number, respectively; $c$ is the velocity of light; and $a$ and $b$ are the minimum and maximum diameter of the corrugated-wall wave guide.

Equation (1) and an approximate solution of (2) for the $TM_{01}$ and $TM_{02}$ modes are plotted in Fig. 2. The two low-order TM modes are of interest since the axial electric field associated with these modes maximizes on axis, where the beam is located. Interaction between the slow-wave circuit and the beam can be expected whenever there is intersection between the negative-energy space charge wave and the structure dispersion relations as indicated by *A* and *B* in Fig. 2. It is possible to deduce important properties of the periodically loaded guide directly from the

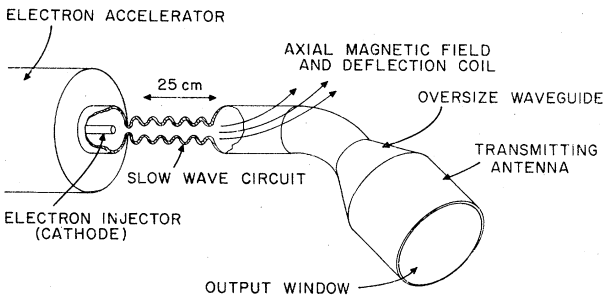


FIG. 1. Schematic of the experimental microwave generator (BWO).

feature of periodicity; i.e., $\omega$ versus $k$ is a periodic function with period $2\pi/L$, where $L$ is the corrugation period. Both points $A$ and $B$ in Fig. 2 represent operation of the device as a BWO. The interaction frequency is deduced from simultaneous solution of Eqs. (1) and (2). The transverse dimensions of the corrugated guide (5 cm o.d., 4 cm i.d.) and the period of the corrugation (1.6 cm) were chosen from consideration of narrow-band frequency generation.

Since the microwave power propagates toward the cathode, the working space of the corrugated wave guide was separated from the beam injector by a narrow neck which is beyond the cutoff frequency of the $TM_{01}$ mode. This arrangement makes it possible to extract the electromagnetic radiation in the direction of the electron motion, through a transmitting horn. The bend in the wave guide, as well as the magnetic deflection system (see Fig. 1), formed a beam dump and also prevented cathode disintegration particles from hitting the Lucite output window.

Measurement of power and frequency were performed using a single-mode dispersive line[15] along with calibrated attenuators and detectors. Figure 3(a) illustrates the observed emission frequency as a function of the beam injection velocity. (The beam drift velocity is somewhat lower.) The experimental results are also compared with the frequency calculated earlier using Eqs. (1) and (2). The relatively good correspondence probably indicates that the emission is in the two lowest-order TM modes, namely $TM_{01}$ and $TM_{02}$. No correlation has been found between the frequency of the radiation and the axial magnetic field strength in which the device was immersed. The radiation power, however, is strongly dependent on the magnetic field strength as shown in Fig. 3(b). Furthermore, below the critical magnetic field (at which the emission power is

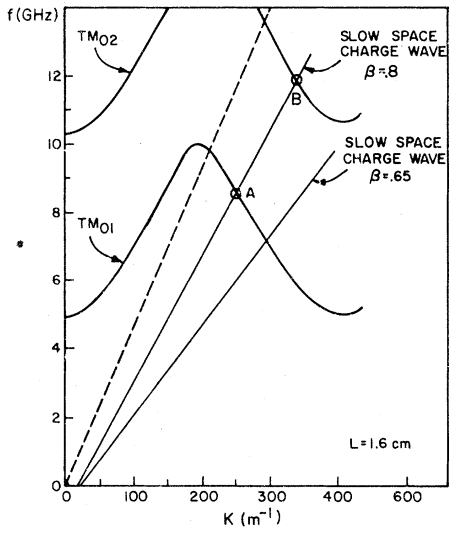


FIG. 2. Dispersion curves for the slow-wave structure and slow space charge wave on the beam. $A$ and $B$ are the points of interaction.

maximum), the dominant mode is $TM_{02}$, while above it $TM_{01}$ is dominant. The peak in the emission could be associated with one of two processes:

(a) At peak emission conditions the electron motion in the uniform axial magnetic field and the spatially varying electric field $E_r(Z)$ approximately satisfies the condition $(2\pi/L)V_{\parallel}=\Omega_c/\gamma$, with $\Omega_c=eB/m$. Consequently the possibility of a resonant transfer of electron motion from axial to the transverse sense maximizes close to the peak in emission. (b) Part of the falloff in radiated power above the resonance may be due to changes in impedance in the diode electron gun. This impedance is shown as a function of the magnetic field strength in Fig. 3(c). The increase is associated with the design of the injector system and is determined by the intersection of the electron orbits with the neck in the ripple structure. In this case the peak in the radiated power would be attributed to a falloff in the beam current on either side of the peak, the low-magnetic-field dropoff resulting from an insufficiently strong magnetic field to contain all of the beam and the high-field dropoff occurring as a result of the beam impedance increase.

In order to avoid breakdown on the air side of the output window, a 15-cm aperture horn was used. Even so, it is somewhat surprising that a horn of this size can handle 500 MW without microwave breakdown on the window[16] (time-integrated photography of the output window showed

no sign of breakdown and the microwave radiation pulse lasted for the full beam duration). It is therefore believed that the wave-guide bend and the primitive transmitting horn cause a mode conversion in the oversize guide used, thereby smoothing the fields due to the wave on the output window and hence increasing the power handling capabilities of the window. This is strongly supported by the presence of both vertical and horizontal polarization in the radiated power, whereas only one polarization can be expected to be present for a pure TM mode at the location of the receiving antenna. At present only a rough radiation pattern is available, indicating two main lobes of 20 deg each, with minimum on axis. Measurements of the emission bandwidth are limited by the resolution of the dispersive line which is about 4% at 10 GHz. No information is available concerning emission in higher modes or harmonics. The base pressure was less than $3\times10^{-4}$ Torr and it is likely that background plasma effects should also be considered.

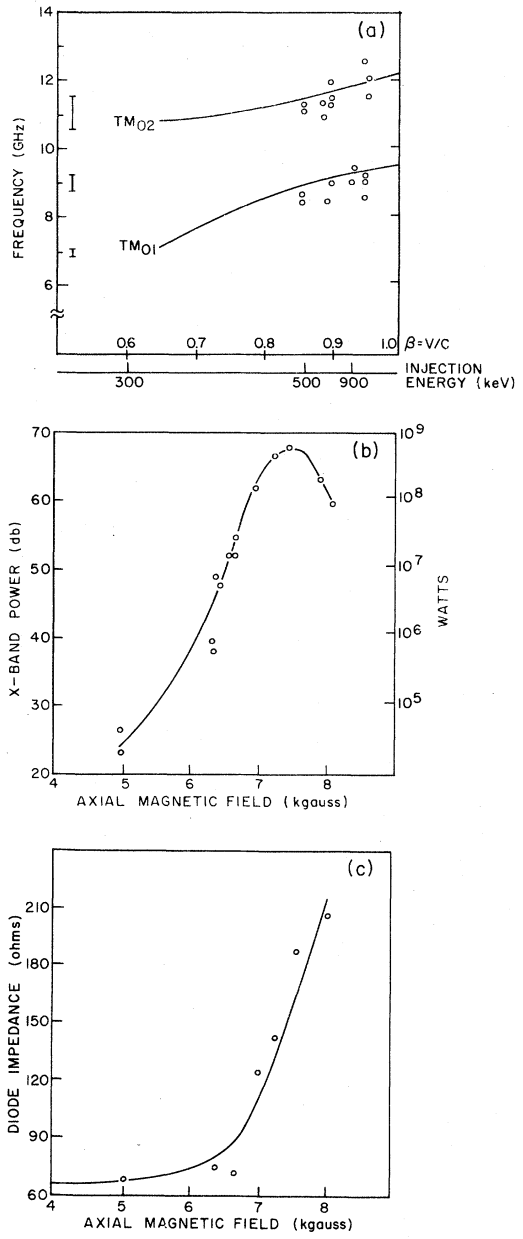


FIG. 3. (a) Microwave frequency as a function of beam velocity, assuming that the injection velocity equals the drift velocity. Solid lines, calculated values; dots, measured values. (b) Microwave power as a function of the axial magnetic field strength. (c) Diode impedance as a function of the axial magnetic field strength.

On the basis of the experimental results we can rule out the negative-energy cyclotron-wave instability as a dominant mechanism. The results are also consistent with the coupling of a negative-energy space charge wave on the beam to a TM mode in the guide. The variation in the radiated power with the magnetic field strength is probably associated with the change in the beam injection parameters with field strength. The peak in radiated power does, however, occur at the resonance condition for electron motion through the rippled structure and could therefore be associated with a fast cyclotron-wave instability, where the resonance motion effects produce free energy to drive the instability.

The efficiency of conversion from beam injection energy to radiated energy essentially follows the curve shown in Fig. 2, peaking at 17% efficiency. The conversion efficiency from beam drift energy to microwave power is somewhat higher and not known at this time. Based on the figures given[17] for breakdown field strengths in superconducting cavities it would seem that higher powers can be achieved without gas breakdown. Better vacuum systems and careful design of output windows are needed, however, to achieve these powers.

The authors are grateful to E. Ott of Cornell University and V. Granatstein of the Naval Research Laboratory for helpful discussions. This work was supported in part by the National Science Foundation and in part by the U. S. Office of Naval Research.

[1]J. Nation, Appl. Phys. Lett. 17, 491 (1970).
[2]E. Ott and W. Manheimer, Phys. Fluids 17, 463 (1974), and to be published.

[3]M. Friedman and M. Herndon, Phys. Rev. Lett. 21, 491 (1970).
[4]M. Friedman and M. Herndon, Phys. Rev. Lett. 29, 55 (1970).
[5]Y. Carmel and J. Nation, J. Appl. Phys. 44, 5268 (1973).
[6]M. Friedman and M. Herndon, Phys. Fluids 16, 1982 (1973).
[7]Y. Carmel and J. Nation, Phys. Rev. Lett. 31, 806 (1973).
[8]V. Granatstein, to be published; M. Friedman and D. A. Hammer, Appl. Phys. Lett. 21, 204 (1972).
[9]V. Granatstein, M. Herndon, Y. Carmel, and J. Nation, to be published, and Bull. Amer. Phys. Soc. 18, 1354 (1973).
[10]N. Kovalev *et al.*, Pis'ma Zh. Eksp. Teor. Fiz. 18, 232 (1973) [JETP Lett. 18, 138 (1973)].
[11]V. Granatstein and P. Sprangle, private communication.
[12]M. Read and J. Nation, Appl. Phys. Lett. 23, 426 (1973).
[13]G. Branch and T. Mihran, IRE Trans. Electron Devices 2, 3 (1955).
[14]See, for example, C. Johnson, *Fields and Wave Electrodynamics* (McGraw Hill, New York, 1965), Chap. 7.
[15]J. Nation, Appl. Phys. Lett. 21, 491 (1970).
[16]See, for example, A. D. MacDonald, *Microwave Breakdown in Gases* (Wiley, New York, 1966).
[17]P. Kneisel, O. Skoltz, and J. Halbralter, J. Appl. Phys. 45, 2302 (1974).